The applicability of earth resistivity methods for saline interface definition

Article *in* Journal of Hydrology · January 2006

DOI: 10.1016/j.jhydrol.2005.05.004

Malcolm Ingham
Victoria University of Wellington

Jack Mcconchie
Opus International Consultants Ltd

Available online at www.sciencedirect.com
SCIENCE DIRECT®
ELSEVIER
Journal of Hydrology xx (2005) 1–12
Journal of Hydrology
www.elsevier.com/locate/jhydrol

The applicability of earth resistivity methods for saline interface definition

S.R. Wilson[a,1], M. Ingham[b,*], J.A. McConchie[a,2]

[a]School of Earth Sciences, Victoria University, P.O. Box 600, Wellington, New Zealand
[b]School of Chemical and Physical Sciences, Victoria University, P.O. Box 600, Wellington, New Zealand

Received 16 June 2004; revised 18 April 2005; accepted 9 May 2005

Abstract

Direct current resistivity traversing has been used to characterise the nature of the saline interface at Te Horo on the Kapiti Coast in New Zealand. The results show that the interface in the vicinity of the settlement, which relies on bores for potable water, has intruded inland 10 m further than in undeveloped areas. Resistivity traversing has been particularly successful in defining subsurface areas of higher salinity by providing a two-dimensional image of the bulk resistivity structure. The results of the resistivity surveys are supported by bore water chemistry, which show evidence of saltwater mixing. Bores on beachfront properties have concentrations of up to 1% seawater. A resistivity formation factor has been derived to allow the pore fluid resistivity to be estimated for future coastal surveys. The results also illustrate the problems associated with using standard models to predict the location of the saline interface when small amounts of diffusive mixing occur.

Keywords: Saline intrusion; Resistivity traversing; Earth resistivity; Formation factor; Coastal aquifers

1. Introduction

Eighty percent of New Zealand's freshwater resource is underground, and most of this is in aquifers bounded on one side by the coast. The population pattern and heavy reliance on agriculture and horticulture mean that most groundwater users tap into coastal aquifers that supply over 50% of New Zealand's groundwater (Lincoln Environmental, 2000). In the lower North Island for example, over 12,000 bores tap this water resource to support communities, commerce, and agriculture (White, 2001). A similar dependence on coastal groundwater exists in many other countries (IAH, 2003). These aquifers are, however, extremely vulnerable to salinisation from saltwater intrusion which is arguably the most common and widespread contamination problem in aquifers around the world.

Groundwater is therefore an important resource in New Zealand. It is used extensively for domestic

* Corresponding author. Tel.: +64 4 463 5216; fax: +64 4 463 5237.

E-mail addresses: swi@marlborough.govt.nz (S.R. Wilson), malcolm.ingham@vuw.ac.nz (M. Ingham), jack.mcconchie@vuw.ac.nz (J.A. McConchie).

[1] Present address: Marlborough District Council, P.O. Box 443, Blenheim, New Zealand. Fax: +64 4 463 5186.

[2] Fax: +64 4 463 5186.

0022-1694/$ - see front matter © 2005 Published by Elsevier B.V.
doi:10.1016/j.jhydrol.2005.05.004

water supply with approximately 25% of the country's population relying solely on groundwater for potable water (Davies, 2001). As the majority of New Zealand's population lives in coastal areas, and as the demand for residential property continues to grow, increasing stress is being placed on coastal aquifers. If groundwater abstraction exceeds recharge the sustainability of many coastal communities reliant on groundwater for potable water is at risk from seawater intrusion. To date, however, there have been no studies published on the characteristics of the saline interface along New Zealand coastlines. In this paper we describe the results of a study of the applicability of direct current resistivity methods for characterising the saline interface under typical conditions.

The study area is located on the Kapiti Coast approximately 65 km north of Wellington (Fig. 1). During summer both the surface and groundwater resources of this area are already stressed, and the situation is likely to worsen with ongoing development. This is because properties outside urban areas do not have a reticulated water supply and are usually reliant on bores for potable water. The Te Horo Beach settlement, typical of the Kapiti Coast, is becoming a popular location for holiday houses and 'lifestyle blocks', and an increasing number of bores therefore tap the coastal aquifer.

2. Aquifer stratigraphy and hydraulic properties

The unconfined aquifer at Te Horo has an area of $\sim 22\ \mathrm{km}^2$. It is bounded to the north by alluvial terraces formed by the Otaki River, and to the east by a 6500-year old marine escarpment. The aquifer lies beneath what is commonly referred to as the 'Holocene coastal plain' which consists of an interfingered alluvial and marine terrace surface which dips gently (2–3°) to the west. The surface is overlain by a sequence of sand dunes, within which four phases of activity are apparent. Dune relief becomes progressively lower, and dune extent smaller and less significant, towards the coast (Fig. 1).

The aquifer is composed of a wedge of unconsolidated postglacial Holocene sediments derived from Mesozoic greywacke basement rocks (Heron and van Dissen, 1992). The sediments thicken towards the coast to reach a maximum thickness of ~ 25 m (Fig. 2). The upper half of the stratigraphic assemblage is composed of fluvial or deltaic gravels,

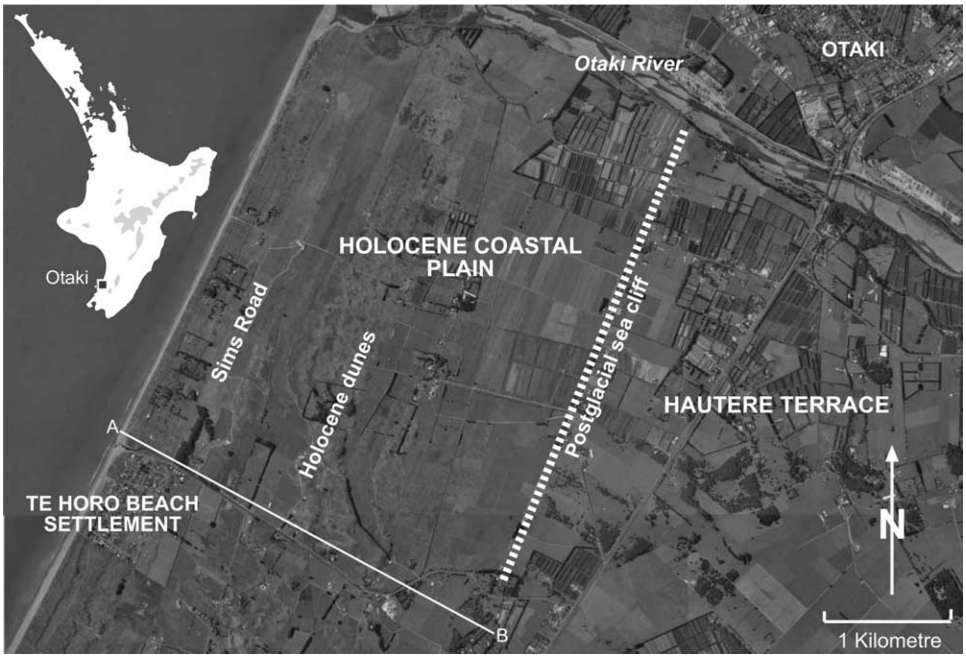

Fig. 1. Location of the study area in the lower part of the North Island of New Zealand. Line AB marks the cross-section shown in Fig. 2.

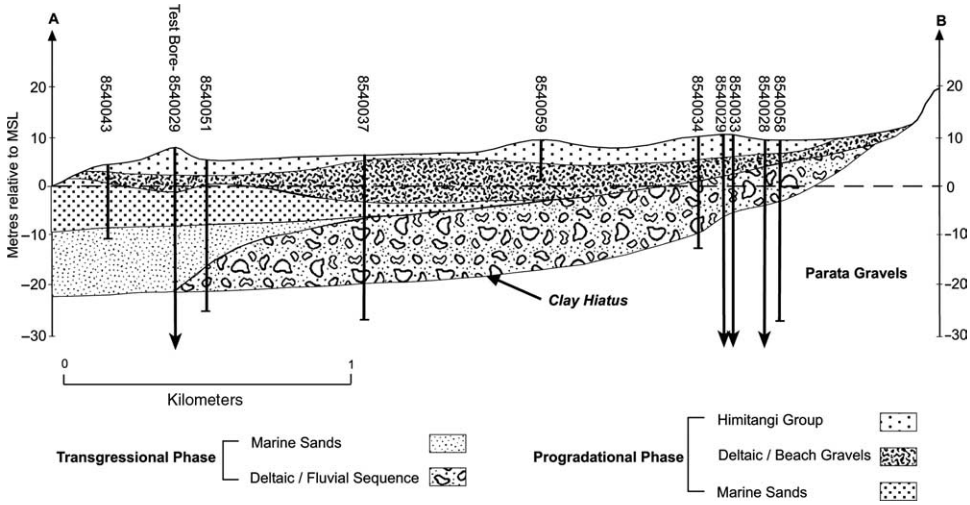

Fig. 2. Stratigraphic cross-section at Te Horo Beach. Solid lines indicate the locations and depths of boreholes from which the cross-section has been constructed.

and marine sands deposited on a prograding coastline. These are overlain by sand dunes and interdune swamp deposits. The lower units are fluvial or deltaic gravels, and marine sands deposited during the last postglacial marine transgression. The base of the aquifer is distinguished by a prominent clay and peat layer, up to 1 m thick, which pinches out to the west. Below this are older, mostly poorly sorted fluvial outwash fans deposited during successive glacial-interglacial events during the Quaternary (Fleming, 1972; Brown, 2003). Bore logs show that near the coast the aquifer is composed of homogeneous water bearing sands; with occasional gravel, wood, and pumice, to a depth of over 20 m. The nature of the depositional environment means that the sands contain no clay (Fig. 3). The marine sand units, which form the host medium for the saline interface on the Kapiti Coast, extend ∼40–100 m inland.

Te Horo has a mild and sub-humid climate. Sunshine hours range from 1850 to 2050 per year, and mean monthly temperatures vary from 11.7 to 20 °C. The prevailing wind comes from the west to northwest, with south to southwest being the next most prevalent direction. Because of this the Tararua Range to the east creates orographic rain in inland areas. Rainfall isohyets therefore follow the coastline, with the major variation being in a west–east direction (Wellington Regional Council, 1994). Mean monthly and annual rainfalls at Te Horo are low (Table 1). Data from the Puruaha rain gauge, located 100 m southwest of Te Horo Beach Road and 30 m from the coast, over 7 years indicate a mean annual rainfall of only 371 mm. Rainfall is evenly spread throughout the year with only slightly less during summer (January–March). While pan evaporation data are not available for Te Horo they were recorded at Levin (35 km to the north) and Paraparaumu (20 km to the south) over the same period as rainfall. Data for Te Horo are estimated as the mean of the other two stations since it lies midway between these two stations and there is little north–south variation (Table 1). Although pan evaporation rates over-estimate actual evapotranspiration losses these data indicate a water stressed area with little potential for rainfall recharge of the aquifer. The majority of recharge occurs via infiltration from local rivers, and rainfall recharge through the Hautere terrace located in the higher rainfall area to the east.

The hydraulic conductivity of the marine sands has been estimated from slug tests as 2.5 m/day (Wilson, 2003). However, analysis of driller's pumping tests suggests that there is considerable variability in the hydraulic conductivity within the sand unit. The mean

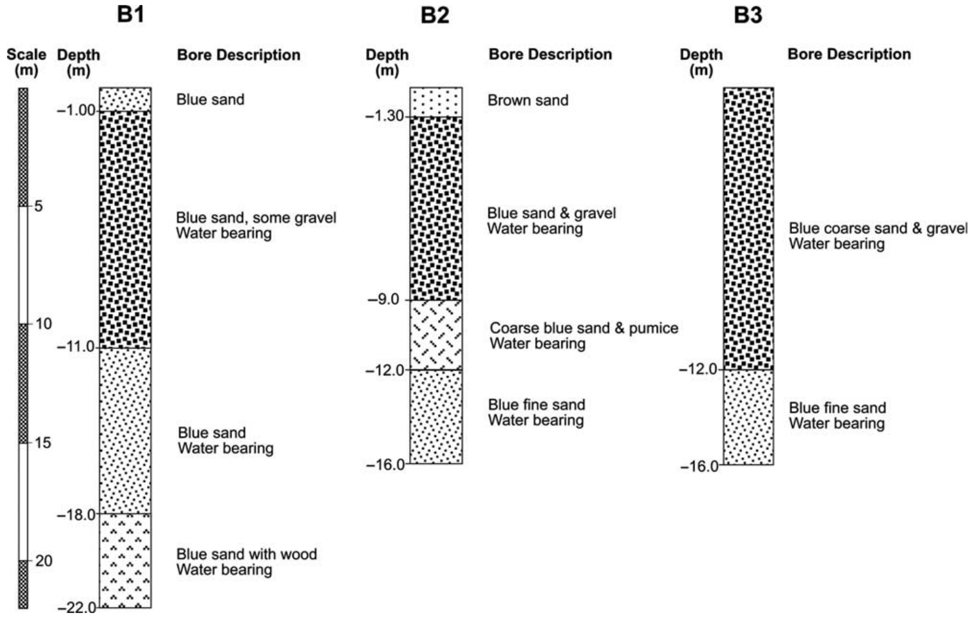

Fig. 3. Bore logs showing that the aquifer is composed of homogeneous water bearing sand to a depth of over 20 m. The locations of the bores are shown in Fig. 5.

hydraulic gradient has been estimated at 0.006 ± 0.004. These data give a mean aquifer flow velocity of 0.015 ± 0.010 m/day (Wilson, 2003).

The stratigraphy, climate, hydrology, hydrogeology, and land use of the area mean that the configuration and dynamics of the aquifer at Te Horo are relatively simple. The lack of intensive water extraction also means that it is likely that the aquifer is in equilibrium. These factors make the use of resistivity and general interpretative models very effective in investigating the saline interface in this study area.

3. Dc resistivity techniques

Direct current (dc) resistivity is one of a number of geophysical techniques commonly used to measure the bulk resistivity of the ground. Within an aquifer the bulk resistivity obeys an empirical law first proposed by Archie (1942). This relationship may be expressed as,

$$\rho = a\varphi^{-m}S^{-n}\rho_{\mathrm{f}}$$

where ϕ is the porosity of the rock formation, S is the degree of saturation, a, m and n are constants that

Table 1
Average monthly rainfall, pan evaporation, and therefore effective precipitation data for Te Horo Beach for the period 01/01/1995–31/10/2002

	Jan	Feb	Mar	Apr	May	Jun	Jul	Aug	Sep	Oct	Nov	Dec	Total
Rainfall (mm)													
Mean	19	25	24	27	31	34	35	31	29	48	35	33	371
Min	6	9	12	10	8	17	11	19	9	18	9	18	146
Max	37	46	33	53	48	54	65	47	38	110	52	53	636
Evaporation (mm)													
Levin	115	92	84	57	47	36	40	47	57	71	90	102	838
Paraparaumu	127	106	99	66	59	45	47	56	66	87	111	124	993
Mean (Te Horo)	121	99	92	62	53	41	44	51	62	79	101	113	916
Effective precipitation (mm)	−102	−74	−68	−35	−22	−7	−9	−20	−33	−31	−66	−80	−545

depend upon the formation, and ρ_f is the resistivity of the pore fluid. Archie's Law shows therefore that the bulk resistivity ρ of a water bearing formation containing no clay, such as in the current study, depends crucially on the resistivity of the pore fluid ρ_f. This is because the resistivity of the fluid is generally much lower than that of the solid grains in the matrix. Since, 'matrix conduction' is negligible, the electric current passes almost entirely through the fluid phase.

For this reason resistivity methods are valuable to many hydrological situations. Measurements obtained from dc methods have previously been employed in a number of groundwater studies (e.g. Aaltonen and Olofsson, 2002; Albouy et al., 2001; Broadbent and Callander, 1991; Devi et al., 2001; Ebraheem et al., 1997; Karlik and Kaya, 2001; Sandberg et al., 2002). The most frequently used technique has been vertical electric sounding (VES). In VES an electric current (I) is introduced into the ground through two outer electrodes and the resulting potential difference (ΔV) is measured between two inner electrodes. An apparent resistivity, calculated from I, ΔV and the electrode geometry, represents the average resistivity of the ground down to the median depth of current penetration. By increasing the distance between the outer electrodes current can be made to penetrate deeper into the ground. A sequence of measurements made with increasing current electrode separation can therefore be modelled in terms of the variation of bulk resistivity with depth.

An alternative technique is that of resistivity traversing. This technique uses a large number of electrodes arranged in a line with a common basic spacing, a (Fig. 4). In the simplest geometry (that of a Wenner array) current is injected into, and taken from, the ground through electrodes 1 and 4. The potential difference is measured between electrodes 2 and 3 (Fig. 4). The resulting value of apparent resistivity may be associated with a location below the midpoint of the four electrodes (e.g. A for electrodes 1–4). By selecting different combinations of electrodes, and using multiples of the base electrode separation (i.e. increasing the separation of the current electrodes and therefore the depth of current penetration), a cone of measurements is obtained. This is generally plotted as a pseudosection in which the vertical axis is related to the electrode spacing. The data may also be modelled two-dimensionally (Loke and Barker, 1996; Loke, 2000) to give an image of the lateral and vertical variations in resistivity. Additional lateral coverage may be obtained by moving the entire electrode array.

4. Vertical electrical soundings

Reconnaissance VES surveys to locate the extent of the saline interface were performed using the Schlumberger array geometry (e.g. Lowrie, 1997). Individual soundings were made with electrodes aligned parallel to the beach so that collectively the

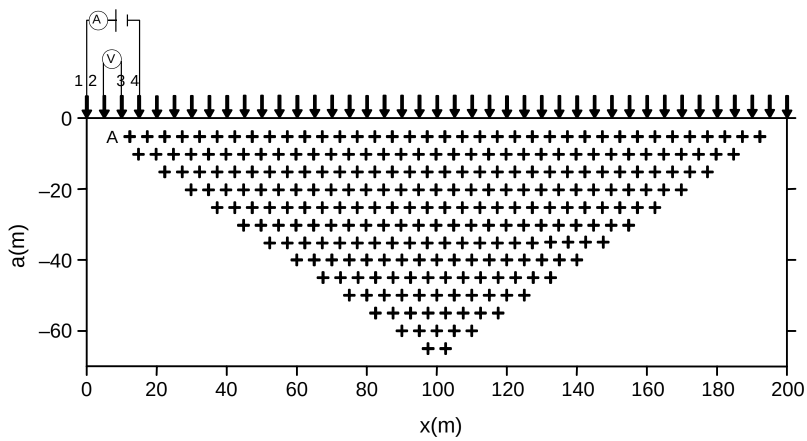

Fig. 4. Geometry of a dc resistivity traverse using 41 electrodes at 5 m separations. Electrode locations are marked by the arrows. Crosses mark the inferred locations at which measurements are made as described in the text. A marks the measurement location derived using the first four electrodes.

soundings would show the variation of resistivity with distance from the coast. The locations of soundings are shown in Fig. 5. Soundings SA-SE were carried out at ∼25 m intervals from the mean high tide mark. Other soundings (S1–S5) were made to both check for the reliability of the structure derived from the resistivity traverses discussed below, and to determine the structure further inland than the extent of the traverses.

Fig. 6 shows the result of a single VES carried out at a distance of ∼65 m above the mean high tide (MHT) mark. The measured apparent resistivity data are shown as squares while the smooth curve through the data represents the derived layered model. The model is composed of a series of layers of constant resistivity. Thus, the data in this case can be modelled

Fig. 5. Location of dc resistivity traverses T1, T2 and T3. C, D, M, S and Sp mark the locations of bore holes used for water quality analyses, and estimation of the formation factor. The bore logs shown in Fig. 3 are marked as B1–B3, while the location of resistivity soundings are prefixed ‘S’.

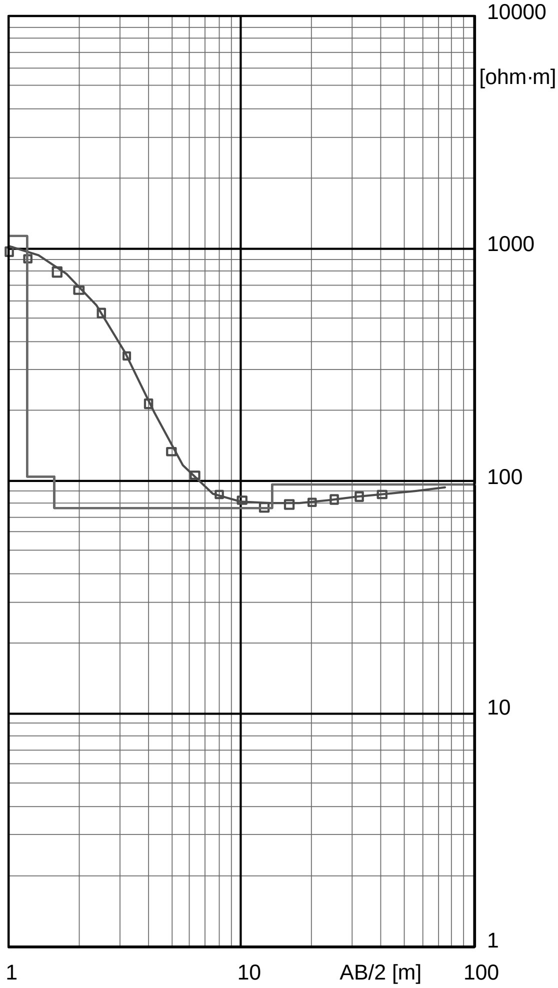

Model Resistivity [ohm·m]	Thickness [m]	Depth [m]
1128	1.2	
105	.38	1.2
76	12	1.6
97		14

Fig. 6. Schlumberger dc resistivity sounding from Te Horo beach. Measured data are shown by the squares, the smooth line through the data points shows the calculated response from the inferred resistivity structure.

by a surface layer of 1128 Ωm, underlain by successive layers of 105, 76 and 97 Ωm at depths of 1.2, 1.6 and 14 m, respectively. These results are typical of all surveys conducted inland of the interpreted saline interface. Comparison of the resistivity model with the bore logs (Fig. 3) suggests that the boundary between the high resistivity surface layer and the underlying less resistive layers is associated with the water table rather than marking any litho logical boundary. Only minor variations in resistivity occur beneath the water table. These earth-resistivities of 80–120 Ωm are consistent with the expected value for sands saturated with freshwater (e.g. White, 1985). Results for surveys conducted within 50 m of MHT returned lower resistivities (∼50 Ωm or less) indicating increased salinity. However, although the VES measurements show a variation in bulk resistivity with distance from the coast that may be related to the degree of saline mixing, they do not give a detailed picture of either the location or structure of the saline interface.

5. Resistivity traverses

Having located the approximate position of the saline interface, resistivity traversing was used to refine its location, and shape, along three profiles. Three traverses perpendicular to the beach were chosen, at Te Horo Beach settlement (T3), approximately 2 km to the north-east (T2), and halfway between these two (T1) (Fig. 5). A basic electrode spacing of 5 m was used, with a maximum electrode separation of 35 or 40 m. Measurements were made using an ABEM SAS 300C resistivity meter in association with a manual electrode switching system constructed at Victoria University of Wellington. Along T1 and T2 the traverses extended from the beach to ∼180 m inland. At T3, within the settlement, restricted access meant that the traverse could only be extended

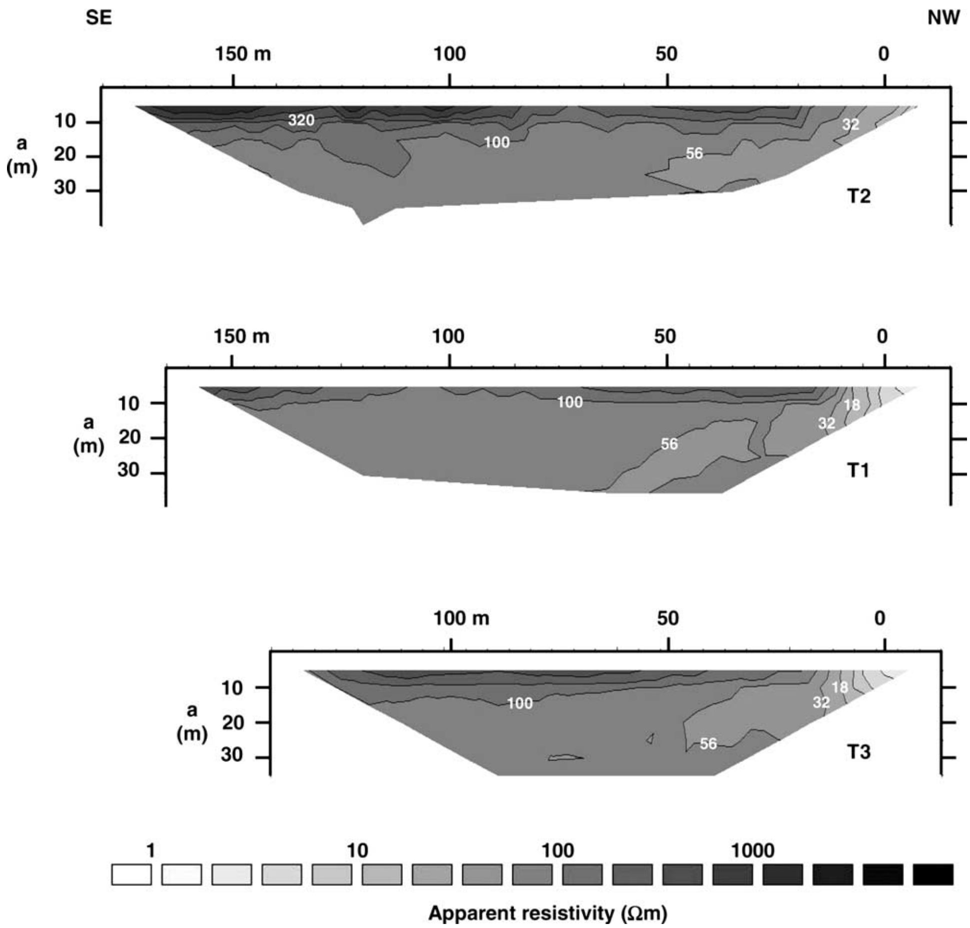

Fig. 7. Pseudosections of apparent resistivity measured for the three traverses T1, T2 and T3. Mean High Tide (MHT) is at 0 m horizontal.

150 m inland. The data obtained from these traverses are shown in Fig. 7 as pseudosections of $\log_{10}(\rho_a)$. The vertical scale represents the electrode spacing used in each set of measurements and the horizontal scale is in terms of the distance of the centre point of each measurement from mean high tide (MHT) at 0 m.

Each traverse shows a zone of lower apparent resistivity up to ∼50 m inland from the mean high tide mark. Beneath traverse T3, through Te Horo beach settlement, this zone is observed at a shallower depth (narrower electrode spacing) than beneath either traverse T1 or T2. Inland from this region, which is inferred to result from the interaction between saline and fresh water at the saline interface, the apparent resistivity pseudosections are uniform. This suggests that away from the coast the bulk resistivity structure is essentially one-dimensional. On traverse T2 high apparent resistivity values are observed at the south-eastern end of the profile. This section, however, was measured during very dry conditions and electrode contact at the surface was in places poor. This resulted in some extremely high apparent resistivity values for electrode spacings (a) less than approximately 10 m.

The pseudosections shown in Fig. 7 give a general indication of the variation of bulk resistivity beneath each traverse. A two-dimensional model of the actual variation in bulk resistivity can be obtained by performing numerical inversion of the data. The results of such inversions for dc resistivity data, as for other potential field geophysical methods, are however, non-unique. For this reason, and to test the robustness of the results, multiple inversions were performed with slightly different initial parameters using both finite difference and finite element techniques of numerical modelling. Fig. 8 shows

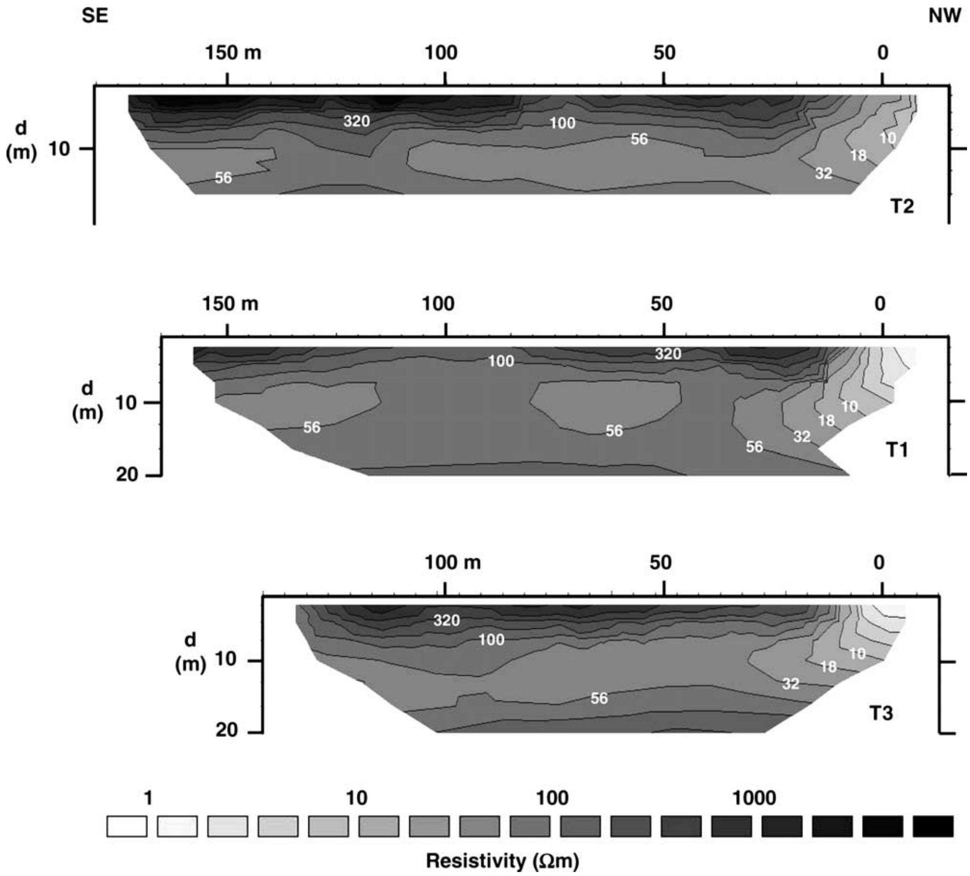

Fig. 8. Inferred two-dimensional resistivity structure beneath the three traverses T1, T2 and T3. Mean High Tide (MHT) is at 0 m horizontal.

the derived two-dimensional models of the bulk resistivity beneath each of the 3 traverses. On each traverse the fit of the derived model to the actual measured data is good. For traverses T1 and T3 overall rms misfits of 4.8 and 5.5% were obtained. The higher rms misfit of 10.9% for traverse T2 reflects the difficulty of modelling the very high apparent resistivity values, measured at small *a*, discussed above.

Unlike discrete vertical electrical soundings, the models presented in Fig. 8 give a continuous spatial image of both lateral and vertical variations in bulk resistivity. Given the uniformity of lithology along the coast as is clearly illustrated by the bore logs shown in Fig. 3, it is assumed that differences between the resistivity models arise from variations in pore fluid resistivity. These variations may be related to the saltwater–freshwater interface. The saline interface is most easily studied by following the zone of low resistivity inland from the MHT. Resistivity values less than 5 Ωm are assumed to represent sand saturated with seawater. The choice of this value of bulk resistivity as a first approximation for defining the saline interface, and the comparison of the interface with classical predictive models such as the Ghyben-Herzberg relation and the Glover (1964) solution are discussed later.

The zone of highest salinity extends furthest inland along traverse T3. This suggests that the saline interface has encroached most at Te Horo Beach settlement as a result of greater pumping for domestic water supply. However, the variation of the interface position on each traverse needs to be treated with caution as it may also reflect tidal effects. The effect of the tide is to move the zone of highest resistivity laterally relative to the high tide mark. This can be seen in traverse T2, which shows the 5 Ωm contour ~7 m seaward of the high tide. On traverses T1 and T3 the 5 Ωm contour is located inland of the high tide mark. To avoid the possibility of mistaking tidal fluctuations for saline intrusion, it is more useful to compare the extent of the low resistivity region rather than just its position. This is similar to studying the dispersion of the interface, which will increase if the freshwater hydraulic head or groundwater flow velocity is reduced by pumping. Each profile shows a distinct 'toe' of low resistivity. This 'toe' is enclosed by the 32 Ωm contour and is seen to extend to a depth of 12–15 m. This contour extends significantly further inland on T3, ~30 m inland of MHT. There is therefore increased saline dispersion beneath traverse T3. This supports the observation above, that the interface has encroached inland at Te Horo Beach settlement by approximately 10 m.

Areas shown on the profiles with a resistivity higher than ~56 Ωm indicate material saturated with freshwater. The resistivity of such material is typically 80–120 Ωm when measured using a Schlumberger VES. Freshwater has a resistivity of 50–100 Ωm (White, 1985), so even areas with a resistivity less than 56 Ωm may represent some degree of saline mixing with freshwater. Extensive areas with bulk resistivity less than 56 Ωm occur on all three traverses. This area is shallowest on traverse T3 measured at Te Horo Beach settlement. This is consistent with the observation that there is an increase in saline dispersion in this area. The discontinuous nature of the 56 Ωm contour in profiles T1 and T2 may represent pockets of fossil seawater, or zones of higher salinity caused by periodic downward flushing of salt spray from the surface. Alternatively, this low resistivity away from the coast may be derived from high solute concentrations associated with mineral dissolution.

Comparison of the models shown in Fig. 8 and the layered models derived from the Schlumberger soundings (e.g. Fig. 6) shows that there is good agreement between the two types of measurements. Apparent differences arise due to the fact that the two-dimensional models of Fig. 8 represent resistivity as varying smoothly rather than being discontinuous across sharp boundaries.

Support for the hypothesis that saline intrusion has occurred beneath Te Horo Beach is provided by geochemical data from boreholes. Measurements of Cl^- ion concentrations from boreholes C and S in Fig. 5 over a 4 year period (Wilson, 2003) show that average concentrations 75 m from MHT on T3 are 3 times higher than they are 500 m inland. A tripling of Cl^- concentration above background levels indicates 1% mixing of seawater (Jones et al., 1999). Peak Cl^- concentrations of 250 mg/L are only just below the maximum level permitted under the New Zealand Drinking Water Standards. Saline intrusion into groundwater also leads to Ca^{++} ion enrichment in the fluid phase (Custodio et al., 1987). Measurements from borehole C also show a clear enhancement of Ca^{++}/Cl^{-} ratios close to the MHT mark.

Comparison of the geochemical data with the bulk resistivity measurements suggest that zones of fresh groundwater, with bulk resistivity from 80 to 120 Ωm, have concentrations of 50 mg/L Cl^{-}, 30 mg/L Na^{+} and total dissolved solids (TDS) of 200 mg/L. In contrast, areas affected by saline intrusion have a bulk resistivity of less than 50 Ωm and concentrations in excess of 100 mg/L Cl^{-}, 60 mg/L Na^{+} and 350 mg/L TDS.

6. Discussion

The formation factor for an aquifer may be defined from Archie's Law, on the assumption that at saturation S is 1, as

$$F = \frac{\rho}{\rho_f} = a\varphi^{-m}$$

This describes, for an aquifer within a homogeneous geological unit, the ratio between the bulk resistivity and the fluid resistivity. Bore log observations of the marine sand unit that hosts the seawater interface at Te Horo indicate that this unit is composed entirely of homogeneous sand, with small amounts of gravel, wood, and pumice. The only clays in the study area form the lower boundary of the aquifer and are therefore below the zone of interest (Wilson, 2003). The formation factor of the marine sand unit can therefore be estimated. The formation factor is a powerful tool in future resistivity surveys in this area as it allows pore-fluid resistivity to be calculated directly from bulk earth resistivity measurements. The relationship can also be used to convert earth resistivity contours into fluid conductivity or TDS contours.

Five boreholes have records of groundwater conductivity that can be used to calculate the formation factor. The bulk resistivity for two of these bores is well constrained by their location on the resistivity profiles (Fig. 1). The bulk resistivity of the other three bores has been estimated from Schlumberger VES conducted nearby. Bulk resistivity values are in fact remarkably homogeneous over a considerable depth range (e.g. the 12 m thickness of 76 Ωm in the model shown in Fig. 6). Variations in resistivity with depth below the water table in the two-dimensional models arise largely from the smooth representation of sharp boundaries. The results (Table 2) give a formation factor of 2.8±0.2. The small uncertainty ensures confidence in the relationship between pore-fluid and bulk resistivity within the marine sand unit. This relationship may be useful for future studies of saline intrusion on the Kapiti Coast where the aquifer is contained within the same marine sands. In such cases this estimate of the formation factor will allow resistivity surveys to provide a good first approximation of pore-fluid resistivity.

Table 2
Measured bore hole fluid resistivities, estimated bulk resistivities, and assessed formation factor

Borehole	ρ_f (Ωm)	Estimated ρ (Ωm)	F
C	14.1	40	2.8
M	19.4	50	2.6
Sp	21.7	60	2.8
S	36.4	100	2.7
D	38.5	110	2.9

The estimated hydraulic conductivity and hydraulic gradient for the aquifer (Wilson, 2003) can be used to predict the location of the saline interface using standard approaches such as the Ghyben-Herzberg relation and the Glover (1964) model. The location of the interface predicted by these models assumes a sharp density boundary between freshwater and seawater. In reality diffusive mixing means that the saline boundary is likely to be distributed, with a gradient in density across it rather than a sharp transition. Where, there has been no saline intrusion the density gradient between fresh and salt water is likely to be steep, and occur over only a few metres. To allow comparison with the resistivity models it is necessary to choose a value of resistivity to represent the boundary. Seawater has a resistivity of approximately 0.3 Ωm. Fresh groundwater typically has resistivities at least a hundred times higher than this value. One option for a resistivity marker to define the location of a sharp saline interface would therefore be an average fluid resistivity of approximately 3 Ωm, or a bulk resistivity (allowing for the formation factor) of 5–10 Ωm. However, as saline intrusion occurs the appropriateness of standard models of the interface becomes much more uncertain. The geochemical data

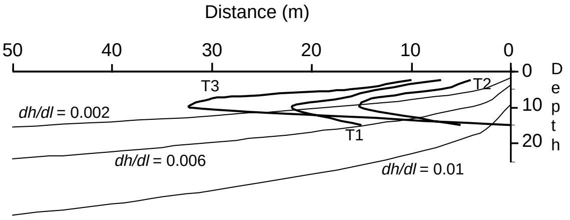

Fig. 9. Calculated location of the saline interface using the Glover (1964) model for three different hydraulic gradients. Also shown (thick lines) are the locations of the 32 Ωm contour beneath the three resistivity traverses.

suggest that, in the present case at least, bulk resistivities of less than 50 Ωm, represent about 1% of saline mixing. This may be an early indicator of the onset of saline intrusion. In such circumstances, the position of the 5 Ωm contour as an indicator of the saline interface is much less important.

The problem discussed above is illustrated in Fig. 9. This shows the location of the saline interface predicted by the Glover (1964) model for three values of the hydraulic gradient, and an assumed hydraulic conductivity of 2.5 m/day. Also shown in Fig. 9 are the positions of the 32 Ωm contour, representing approximately 1–2% of saline mixing, for the three resistivity traverses. Although not explicit in Fig. 9, 5 m inland from MHT the 5 Ωm contour for traverses T1 and T3 closely parallels the predicted saline interface for a hydraulic gradient of 0.002. This value for the hydraulic gradient is, however, solely based on the slope of the surface topography. For traverse T2 the 5 Ωm contour is much closer to the interface predicted using a hydraulic gradient of 0.01, derived from the slope of the base of the unconfined aquifer. Resistivity traversing data can therefore be used to detect the sharp gradient in bulk resistivity associated with the saline interface. The technique is also effective in tracking saline mixing occurring well inland of the predicted interface.

7. Summary and conclusions

Measurement and inversion of three direct current resistivity traverses at Te Horo have allowed the detection of the saltwater/freshwater interface. Beneath a traverse through Te Horo Beach settlement, where there is significant groundwater abstraction, there is clear evidence of saline intrusion. To the north, where development is limited, any intrusion is minor.

These results show clearly the potential of resistivity traversing in mapping and understanding the structure and evolution of the saline interface in coastal aquifers. Although VES data may resolve the one-dimensional resistivity structure beneath a sounding location, any two-dimensional interpretation of the data requires interpolation between discrete measurements. In contrast, resistivity traversing data provide a continuous two-dimensional image of both lateral and vertical variations in resistivity. The significant contrast in the electrical resistivities of saline and fresh water allows direct imaging of a sharp saline interface (inferred here as following the 5 Ωm contour).Diffusive mixing involving as little as 1% seawater can be tracked by the significant reduction in bulk resistivity of the groundwater. Within a given aquifer fluid resistivity values from even a small number of boreholes allows the measured bulk resistivity values to be converted into fluid resistivities. The formation factor defined in this way can then be used to interprete resistivity data from a much wider area.

Acknowledgements

The authors gratefully acknowledge support from the Greater Wellington Regional Council and the University Research Fund of Victoria University of Wellington.

References

Aaltonen, J., Olofsson, B., 2002. Direct current (dc) resistivity measurements in long-term groundwater monitoring programmes. Environmental Geology 41, 662–671.

Albouy, Y., Andrieux, P., Rakotondrasoa, G., Ritz, M., Descloitres, M., Join, J-L., Rasolomanana, E., 2001. Mapping coastal aquifers by joint inversion of dc and TEM soundings—three case histories. Ground Water 39, 87–97.

Archie, G.E., 1942. The electrical resistivity log as an aid in determining some reservoir characteristics. Transactions of the American Institute of Mining & Metallurgical Engineers 146, 54–62.

Broadbent, M., Callander, P.F., 1991. A resistivity survey near Waimakariri river, Canterbury Plains, to improve understanding of local groundwater flow and of the capabilities of the survey method. New Zealand Journal of Geology & Geophysics 34, 441–453.

Brown, L., 2003. Te Horo Beach groundwater investigation bores. Wellington Regional Council Technical Report.

Custodio, E., Bruggeman, G.A., Cotecchia, V., 1987. Groundwater problems in coastal areas. Studies and reports in hydrology, 35, UNESCO, Paris.

Davies, H., 2001. Groundwater and health. In: Rosen, M.R., White, P.A. (Eds.), Groundwaters of New Zealand. New Zealand Hydrological Society, Wellington.

Devi, S.P., Srinivasulu, S., Raju, K.K., 2001. Delineation of groundwater potential zones and electrical resistivity studies for groundwater exploration. Environmental Geology 40, 1252–1264.

Ebraheem, A-A.M., Senosy, M.M., Dahab, K.A., 1997. Geoelectrical and hydrogeochemical studies for delineating groundwater contamination due to salt-water intrusion in the northern part of the Nile delta, Egypt. Ground Water 35, 216–222.

Fleming, C.A., 1972. The contribution of C^{14} dates to the Quaternary geology of the 'Golden Coast', Wellington. Tuatara 7 (2), 197–208.

Glover, R.E., 1964. The pattern of fresh-water flow in a coastal aquifer. In: Sea water in coastal aquifers. US Geological Survey Water-Supply Paper 1613-C, C32–35.

Heron, D.W., van Dissen, R.J., 1992. Geology of the Kapiti Coast (Pukerua Bay to Otaki), Wellington. Contract report CR 1992/19, Wellington Regional Council.

International Association of Hydrologists, 2003. Groundwater—from development to management. Briefing paper for Third World Water Forum, Kyoto, Japan, March 2003.

Jones, B.F., Vengosh, A., Rosenthal, E., Yechieli, Y., 1999. Geochemical investigations. In: Bear, J. et al. (Ed.), Seawater Intrusion in Coastal Aquifers—Concepts, Methods, Practices. Kluwer Academic Publishers, Dordrecht.

Karlik, G., Kaya, M.A., 2001. Investigation of groundwater contamination using electric and electromagnetic methods at an open waste-disposal site: a case study from Isparta, Turkey. Environmental Geology 40, 725–731.

Lincoln Environmental 2000: Information on water allocation in New Zealand. Report for Ministry for the Environment, Report No 4375/1, 107p.

Loke, M.H., 2000. Electrical imaging surveys for environmental and engineering studies. Unpublished Short Training Course Lecture Notes, Geotomo Software, Penang, Malaysia, 65pp.

Loke, M.H., Barker, R.D., 1996. Practical techniques for 3D resistivity surveys and data inversion. Geophysical Prospecting 44, 499–523.

Lowrie, W., 1997. Fundamentals of geophysics. Cambridge University Press p. 354.

Sandberg, S.K., Slater, L.D., Versteeg, R., 2002. An integrated geophysical investigation of the hydrogeology of an anisotropic unconfined aquifer. Journal of Hydrology 267, 227–243.

Wellington Regional Council, 1994. Hydrology of the Kapiti Coast.. wellington Regional Council Report WRC/CI-T/G-94/13.

White, P.A., 1985. Handbook on hydro geological applications of earth resistivity measurements, Water and Soils Publication No. 90. Water and Soil Directorate. Ministry of Works and Development, New Zealand p. 41.

White, P.A., 2001. Groundwater resources in New Zealand. In: Rosen, M.R., White, P.A. (Eds.), Groundwaters of New Zealand. New Zealand Hydrological Society, Wellington.

Wilson, S.R., 2003. The saltwater–freshwater interface, Te Horo Beach, Kapiti Coast. Unpublished MSc Thesis, School of Earth Sciences, Victoria University of Wellington, pp. 147.